Fracture and Impact Properties of Polycarbonates and MBS Elastomer-Modified Polycarbonates

FENG-CHIH CHANG,* JIANN-SHING WU, and LINE-HWA CHU

Institute of Applied Chemistry, National Chiao-Tung University, Hsinchu, Taiwan, Republic of China

SYNOPSIS

Mechanical properties of polycarbonates (PCs) and elastomer-modified polycarbonates with various molecular weights (MW) are investigated. Higher MW PCs show slightly lower density, yield stress, and modulus. The ductile–brittle transition temperature (DBTT) of the notched impact strength decreases with the increase of PC MW and with the increase of elastomer content. The elastomer-modified PC has higher impact strength than does the unmodified counterpart if the failure is in the brittle mode, but has lower impact strength if the failure is in the ductile mode. The critical strain energy release rate (G_c) measured at −30°C decreases with the decrease of PC MW. The extrapolated zero fracture energy was found at M_n = 6800 or MFR = 135. The G_c of the elastomer-modified PC (MFR = 15, 5% elastomer) is about twice that of the unmodified one. The presence of elastomer in the PC matrix promotes the plane–strain localized shear yielding to greater extents and thus increases the impact strength and G_c in a typically brittle fracture. Two separate modes, localized and mass shear yielding, work simultaneously in the elastomer-toughening mechanism. The plane–strain localized shear yielding dominates the toughening mechanism at lower temperatures and brittle failure, while the plane–stress mass shear yielding dominates at higher temperatures and ductile failure. For the elastomer-modified PC (10% elastomer), the estimated extension ratio of the yielding zone of the fractured surface is 2 for the ductile failure and 5 for the brittle crack. A criterion for shifting from brittle to ductile failure based on precrack critical plastic-zone volume is proposed.

INTRODUCTION

Homopolymer matrices can be roughly classified into pseudoductile and brittle. This classification is not strictly defined and is largely based on the performance under practical applications, and therefore the effects from time, temperature, and geometry are ignored. Brittle polymers, such as polystyrene (PS), styrene–acrylonitrile (SAN), and poly(methyl methacrylate) (PMMA), tend to fail with crazing-crack at relatively lower crack initiation and propagation energies. Much research has been carried out to improve the toughness of these polymers by incorporation of a second phase of dispersed rubbery particles. The presence of rubber particles initiates a localized energy-absorbing mechanism from many sites rather than from a few isolated ones. Both interfacial adhesion and optimum particle size (0.1–3.0 μm) are essential depending on polymer matrices. The most well-known example is the high-impact polystyrene (HIPS) that possesses greatly improved toughness over the regular PS. The toughening mechanism of this category is mostly crazing with some shear yielding and cavitation.[1-3] Pseudoductile polymers tend to shear yield with relatively higher crack initiation energy, but with a low crack propagation energy. These polymers are brittle only under conditions of sharp notch, plane strain, and high rates of deformation. Polymers classified in this category are polycarbonate (PC), nylon, poly(vinyl chloride) (PVC), and polyesters. Interfacial adhesion between rubber particles and the pseudoductile matrix is not always required and the optimum particle size is usually smaller (< 0.5 μm). Matrix yield is the main mechanism of energy dissipation in such polymer/rubber blends.

* To whom correspondence should be addressed.

Journal of Applied Polymer Science, Vol. 44, 491–504 (1992)
 CCC 0021-8995/92/030491-14$04.00

There has been a considerable amount of literature on the fracture properties of PCs. This is probably due to its position as one of the most commonly used engineering thermoplastics and the interesting transition behavior that occurs close to ambient conditions. Ductile–brittle transition is a change in fracture behavior from ductile to brittle or brittle to ductile in response to the change of a variable during testing. If the crack initiation appears prior to certain ductile drawing, then it will propagate in a brittle catastrophic manner. If a tear or crack begins after some ductile drawing has occurred, then a ductile failure will result.

Many reasons have been put forward to explain the phenomenon of ductile–brittle transition in glassy polymers, and it seems clear that there is no overriding mechanism responsible for this behavior. Pitman et al.[4] have accounted for the phenomenon observed in PC in terms of a competition between shear yielding and crazing, with shear yielding promoting ductile behavior and crazing causing brittle fracture. Most studies on PC ductile–brittle transition have been carried out by using the conventional Charpy or Izod impact tests. The energy absorbed during testing is not proportional to the notch length in both Charpy and Izod specimens.[5] Diverse studies have reported the factors that influence PC ductile–brittle transition behavior and are listed as follow:

1. Temperature.[4,6,7–19]
2. Rate.[12,15,19,20–22]
3. Notch radius.[7,12–14,16,19,21,23]
4. Specimen thickness.[10,11,15]
5. Annealing.[4,7,12,24–28]
6. Molar mass.[4,12,15,19,22,24,26,29–32]

These factors have important implications for the use of glassy thermoplastics in engineering applications. Similar to the brittle matrices mentioned above, pseudoductile polymers can also be toughened by the introduction of a second soft particulate phase to promote additional shear yielding during the fracture process. Newman and Strella[33] suggested that the principal function of the rubber particles is to produce sufficient triaxial tension in the matrix so as to increase the local free volume and, hence, the shear yielding. Multiple shear yield deformation accompanied by the initiation of cavities is the main toughening mechanism of PVC.[34,35] Matrix yielding has been reported as the main mechanism of energy dissipation in nylon/rubber blends.[36–38] The mechanism of rubber-toughening pseudoductile polymers is not as well defined as that of brittle polymers such as PS and SAN. In spite of a large amount of literature published on PC fracture behavior, only a few have been in the rubber-modified PC. Yee[20] briefly investigated the rubber-toughening mechanism of PC modified with polyethylene (PE) and methyl methacrylate–butadiene–styrene (MBS) elastomer. Riew and Smith[17] studied toughening PC with preformed rubbery particles. Elastomer-modified PC to improve low-temperature performance has been the subject of several U.S. patents.[39–42] The influence of molecular weight (MW) on PC fracture properties is relatively more pronounced than on other matrices. In pursing a better understanding, the effect of MW on PC fracture properties, samples with various MFR from the same manufacturer were employed. Many aspects of PC fracture properties with special emphasis on ductile–brittle transition behavior and the effect of elastomer modification are investigated.

MATERIALS AND METHODS

Nature-grade PC samples with MFR from 3 up to 80 were obtained from the Dow Chemical Co. Except for MFR = 60 and 80, all the samples are commercial-grade products. Molecular weights were determined by GPC using methylene chloride as solvent, and the results are shown in Table I. Densities of the PC pellets were determined by a density-gradient column, model DC-1, from Techne Cambridge Limited, and the results are also listed in Table I. The elastomer employed in this study is Metablend CB-223, a MBS copolymer, in pellet form from M&T Chemical Co. This elastomer is a bimodal core-shell structure with average diameter of 0.08 μm for the small particles and 0.3 μm for the large particles.

Table I Polycarbonate Densities, MFR and MW

PC MFR	M_w (×1,000)	M_n (×1,000)	Density (g/mL)
3	35.9	13.3	1.19740
6	31.5	11.6	1.19820
10	28.2	10.6	1.19850
15	25.1	9.7	1.19860
+1% MBS	—	—	1.19750
+3% MBS	—	—	1.19710
+5% MBS	—	—	1.19550
+10% MBS	—	—	1.18410
22	23.9	9.5	1.19860
60	19.6	8.3	1.19870
80	18.1	7.9	—

The large particles appear to be the agglomeration of small particles according to TEM micrography. Injection molding and extrusion melt blending of PC and elastomer were carried out according to the manufacturer's recommended conditions. Specimens of 6 × 0.5 × 0.125 in. and type I tensile (ASTM D638) were injection molded using a 3 oz Arbury molding machine. The bars were machine notched with a radius of 5.0 or 10 mil using a single tooth cutter. The impact energy was measured by a TMI, model 43-1, impact tester equipped with a temperature-controlled chamber that is able to run from −100 to 150°C. The fractured surfaces were investigated by SEM using a model S-570 SEM from Hitachi Co. Microtome trimming of the yielding portion of the fractured surfaces was carried out by using a Reichert Ultramicrotome and a diamond knife at ambient conditions. The thin section was stained by 1% aqueous solution of OsO_4. Transmission electron microscopy was carried out on a TEM model Jem-100S from Jeol-Technics Co. Tensile tests were carried out according to ASTM D638 with crosshead speed of 10 mm/min on an Instron model 4201.

RESULTS AND DISCUSSION

Tensile Properties

The tensile properties of PCs with various MW are summarized in Table II. The overall trends clearly show that the higher MW PC has slightly lower yield stress and modulus. Molecular weight and its distribution are the important parameters that characterize polymer properties and a certain minimum value for the polymer to behave as a rigid glassy material. Polymer with higher MW needs a relatively longer time to pact into its equilibrium state in a typical injection-molding operation and therefore should possess higher degrees of disorder, greater internal stress, and free volume. That PC density decreases slightly with the increase of MW, as shown in Table I, provides the direct evidence. The density difference between the highest and the lowest MFR PC is about 0.1% (Table I). Golden et al.[30] studied the tensile fracture stress of various MW PCs and reported that low MW PC had very low tensile breaking strength but that the strength increased as the MW was increased and eventually reached a constant level. The M_n of zero-breaking stress of 7500 was thus obtained.[30] The observed variations of yield stress with changes of MW emphasize that PC properties are fairly sensitive to the MW relative to other polymers. Lower yield stress and modulus of the higher MW PC should, in some degree, correlate to its being more ductile. As previously mentioned, the fracture behavior of glassy polymers is controlled by a competition between crazing and bulk shear yielding. Lower yield stress of the higher MW PC is in favor of mass shear yielding. Besides, higher MW polymer usually possesses higher craze stress, which is again in favor of mass shear yielding.

Table II Tensile Properties of Polycarbonates and MBS-modified Polycarbonates

Sample	Yield Stress (MPa)	Percent Elongation	Modulus (MPa)
PC MFR = 3	61.0	85.2	2220
MFR = 6	63.4	90.5	2260
MFR = 10	64.9	88.4	2310
MFR = 15	65.8	97.8	2370
MFR = 22	65.7	85.0	2380
MFR = 60	68.3	41.6	2400
MFR = 80	68.1[a]	—	—
MFR = 80	66.5[b]	4.7[b]	2490
PC MFR = 15			
+1% MBS	65.0	78	2330
+3% MBS	64.3	101	2220
+5% MBS	61.4	102	2170
+10% MBS	57.1	85	2060
PC MFR = 80			
+5% MBS	60.7	33	2210

[a] Extrapolated data.
[b] Experimentally breaking stress and strain.

Molecular entanglements in the polymer network are very important in controlling the fracture behavior. The entanglement density increases as the MW is increased and finally reaches a constant that can explain Golden et al.'s observation.[30] However, the average number of entangled junctions based on a single polymer molecule chain will continuously increase with the increase of MW without any limit, which seems to provide a better explanation of our later results based on fracture energy (G_c). After being modified with 5% MBS elastomer, PC with MFR = 80 becomes ductile in a typical tensile testing. PCs with MFR from 3 to 60 all show the clear yield point and high elongation at break except for the MFR = 60, which has a significantly lower elongation at break. PC with MFR = 15 is a general purpose grade product that was chosen to study the effect of varying quantities of elastomer. Yield stress and modulus decrease with the increase of elastomer contents as would be expected (Table II).

Impact Strength—Effect of Molar Mass and Temperature

Figure 1 illustrates the effect of temperature on impact strength for PCs with various MFRs. The results are fairly consistent within expectations. The PC with lower MFR (higher MW) has lower ductile–brittle transition temperature (DBTT) and higher impact strength in either ductile or brittle failure. Except for the MFR = 80 (and MFR = 60), all the rest of the PCs have the DBTTs below ambient temperature. The stress-whitening yield volume from the surface of the brittle-fractured specimen is microscopic in size and is too small to be measured accurately. Legrand[24] studied the deformed yielding volume of PC in both ductile and brittle fractures and reported that the volume was in the order of 0.08 and 0.00036 mL, respectively. If the impact strength is assumed proportional to the resultant yielding volume, the impact strength (I.S.) of the brittle fracture should be only 0.5% of the ductile fracture instead of 16.7% obtained experimentally (PC, MFR = 15, at 25°C, I.S. = 14.4 ft-lb/in., at −50°C, I.S. = 2.4 ft-lb/in.). Tremendous error could arise without considering other energy-dissipation processes in the brittle fracture, such as crazes, and the excess elastic energy release. Recently, Wu[43] analyzed the energy balance of the rubber-toughened nylon and reported that the impact strength is directly proportional to the volume of the stress-whitened zone, and thus the energy dissipation density is the same for both ductile and brittle fractures. Our study shows that the extension ratio of the yielding volume (discussed below) due to the brittle fracture is significantly higher than the ductile failure. In other words, the energy-dissipation density of the elastomer-modified PC is not expected to be the same from these two types of fractures.

Another interesting comparison is that the impact energy increases for the rubber-toughened nylon[37] and polyacetal[44] over the unmodified ones in both ductile and brittle fractures. This study shows that the elastomer-modified PC actually has less impact energy than does the corresponding unmodified PC if the fracture is in ductile mode. The presence of elastomer in the PC matrix reduces both modulus and yield stress, which is in favor of a more molecular flow in a typical ductile tearing. On the other hand, the presence of elastomer particles reduces the cross-sectional contact area of the PC matrix and therefore hinder the molecular flow. Whether the presence of elastomer in a matrix will increase or decrease of its impact strength in a ductile failure depends on the relative importance of these two competitive factors. Fracture surfaces of PCs have been previously investigated in detail.[11,45] For the ductile and high-energy fracture, the fracture surface appears distorted and irregular. Below the notch, the specimen has yielded a reduction in width, indicating plane–stress fracture conditions. The striations on

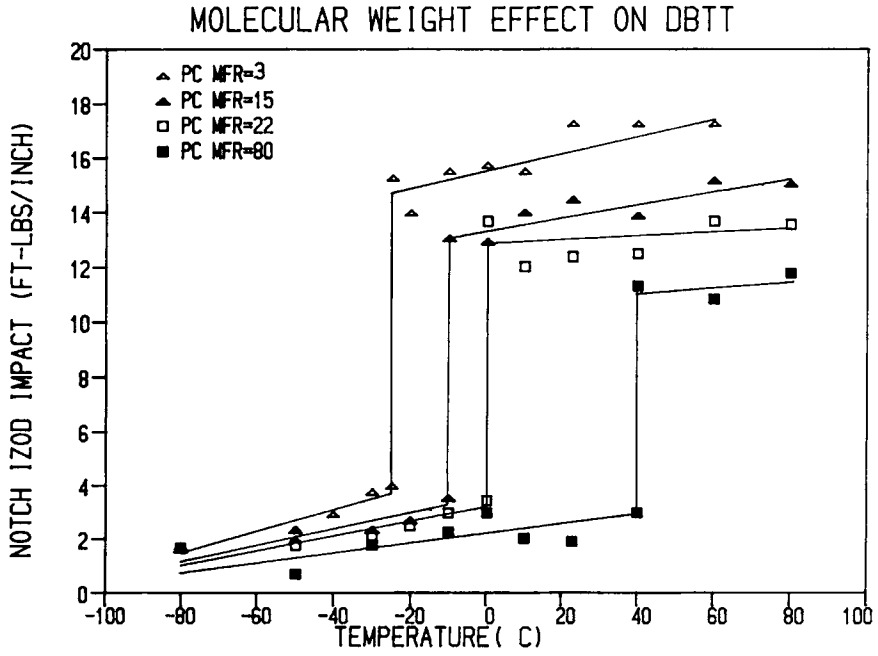

Figure 1 Izod impact strengths of PCs by varying MFR and temperatures.

the fracture surface spread uniformly from the root of the notch following the direction of crack propagation.

Figure 2 shows that the higher MW PC has relatively less density of the striated lines. Figure 2(d) shows the well-defined striated surface with overlapped parabola markings for the PC MFR = 80, which is very similar to zone III of the brittle-fracture surface defined by Hull and Owen[45] except that it is more concentrated and overlapped. Hull and Owen[45] divided the brittle-type fracture of PC into four zones: Zone I associates with the nucleation of

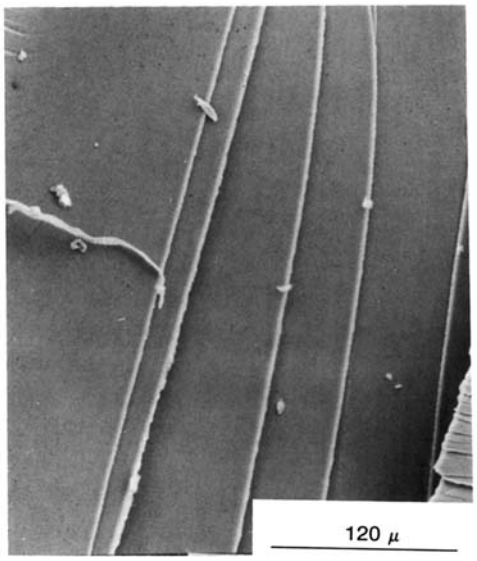

a. MFR = 3,

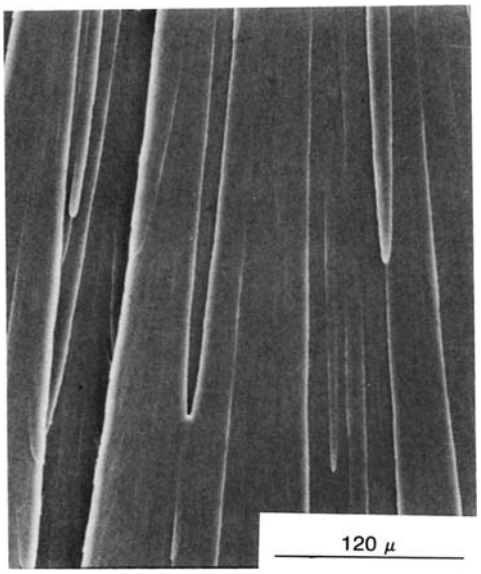

b. MFR = 15,

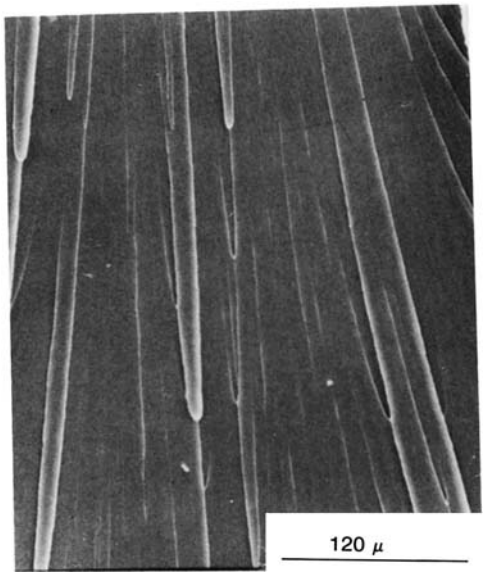

c. MFR = 22,

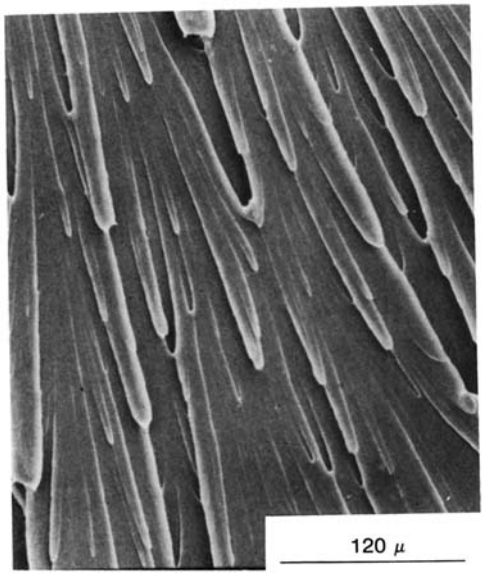

d. MFR = 80

Figure 2 SEM microphotographs of the ductile fractured PC surfaces ×200, at ambient temperature for MFR = 3, 15, and 22, at 60°C for MFR = 80. (a) MFR = 3; (b) MFR = 15; (c) MFR = 22; (d) MFR = 80.

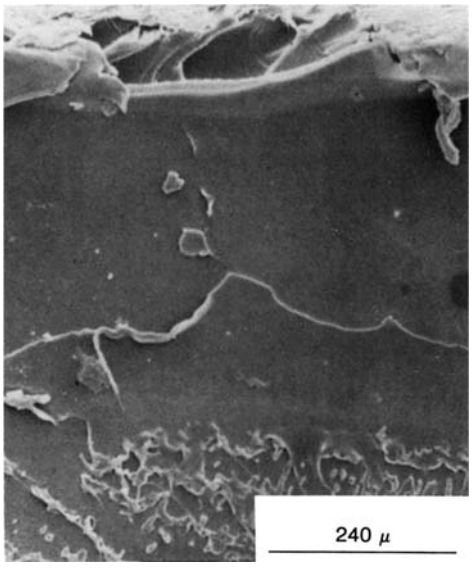

a. MFR = 3,

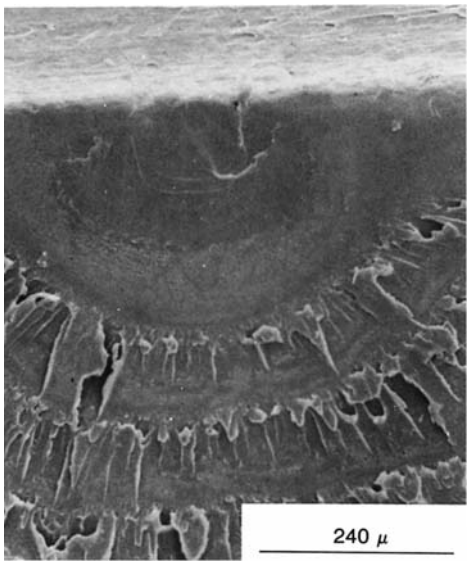

b. MFR = 15,

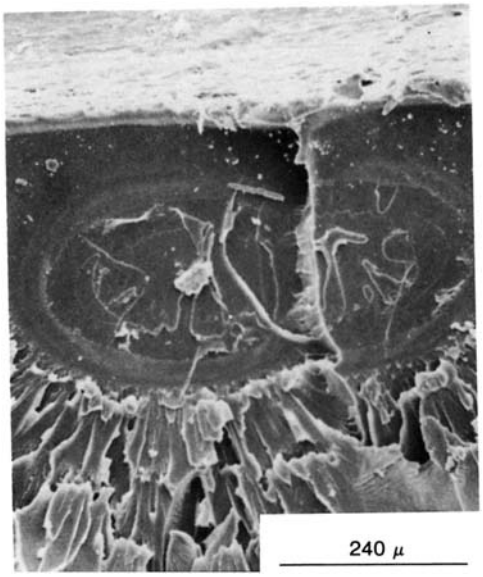

c. MFR = 22,

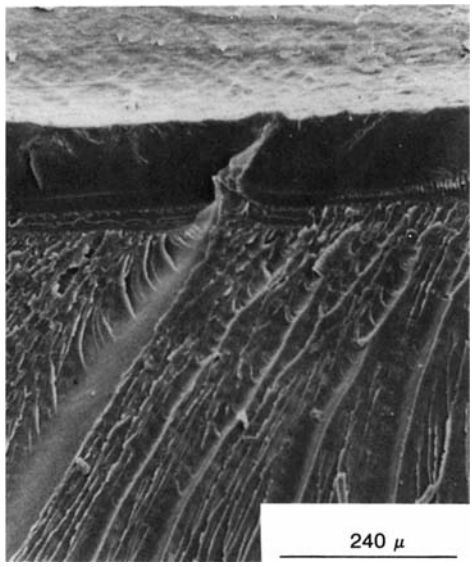

d. MFR = 80

Figure 3 SEM microphotographs of the brittle-fractured PC surfaces ×100, at −60°C. (a) MFR = 3; (b) MFR = 15; (c) MFR = 22; (d) MFR = 80.

a crack below notch. Figure 3 shows the brittle fracture surfaces in an area extending from zone I into zone II according to Hull and Owen's definition.[45] The length of the nucleation zone (zone I) is wider for the PC with higher MW (MFR = 3, 15, 22, 80; d = 0.55, 0.34, 0.38, 0.15 mm). The length of the nucleation zone should correlate with the impact energy in a brittle fracture. The radial markings are totally disappeared for the PC MFR = 80 and replaced with fine striated lines, which reflects much lower impact strength of this low MW specimen relative to others (MFR = 3, 15, 22, 80; I.S. = 2.0, 2.0, 1.8, 0.7 ft-lb/in.). The above observations strongly suggest that the crack initiation is important in determining the total energy absorption in a brittle impact fracture process.

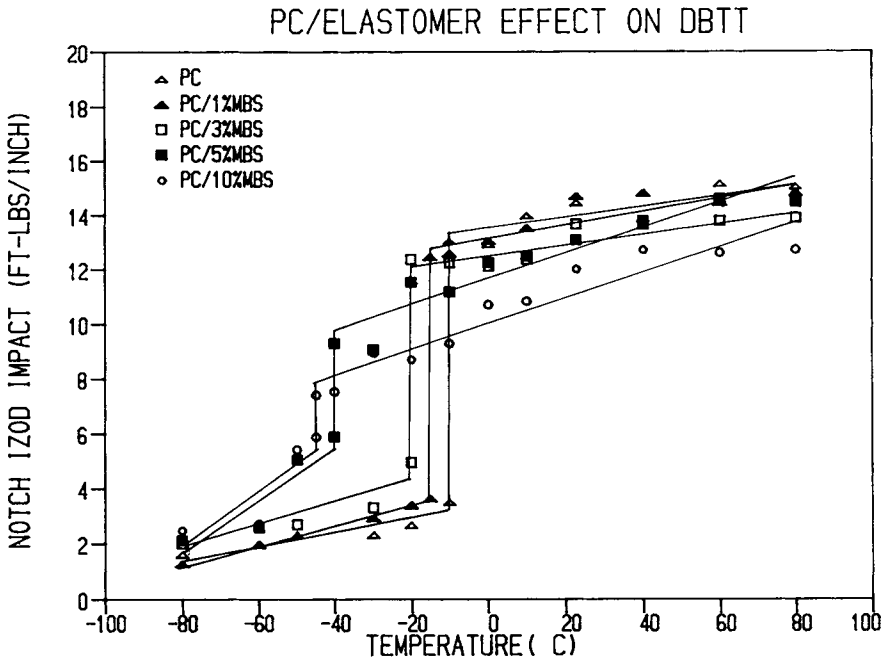

Figure 4 Izod impact strengths of PC MFR = 15 containing various contents of MBS elastomer under different temperatures.

Impact Strength of the Elastomer-Modified Polycarbonates

Figure 4 clearly demonstrates the effect of the elastomer presence on PC impact properties. The presence of more elastomer results in further decrease in the DBTT (Fig. 5) and reduces the energy difference between ductile and brittle fractures at DBTT. The ductile–brittle transition becomes less and less defined as the elastomer content is in-

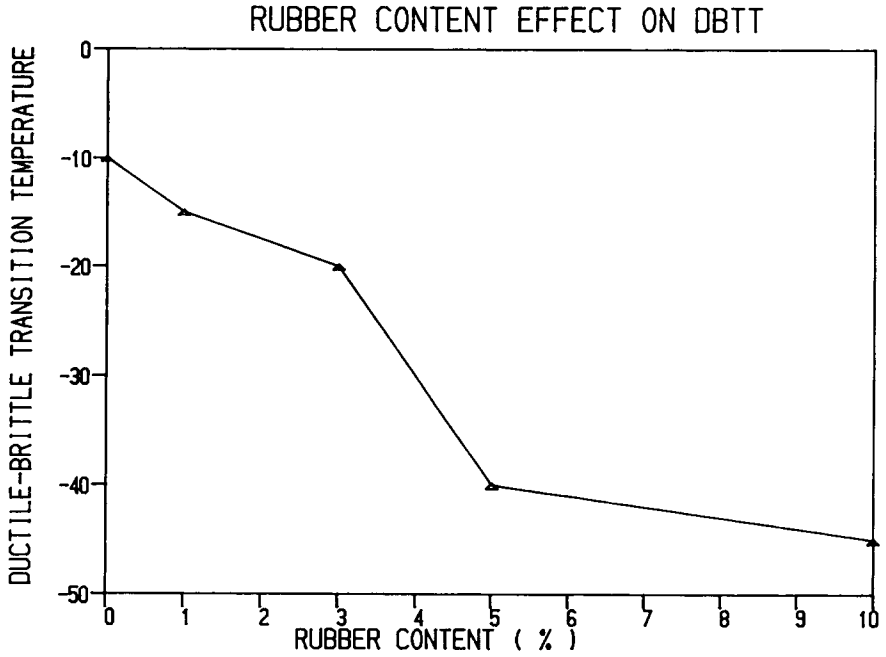

Figure 5 Effect of MBS content on PC DBTT.

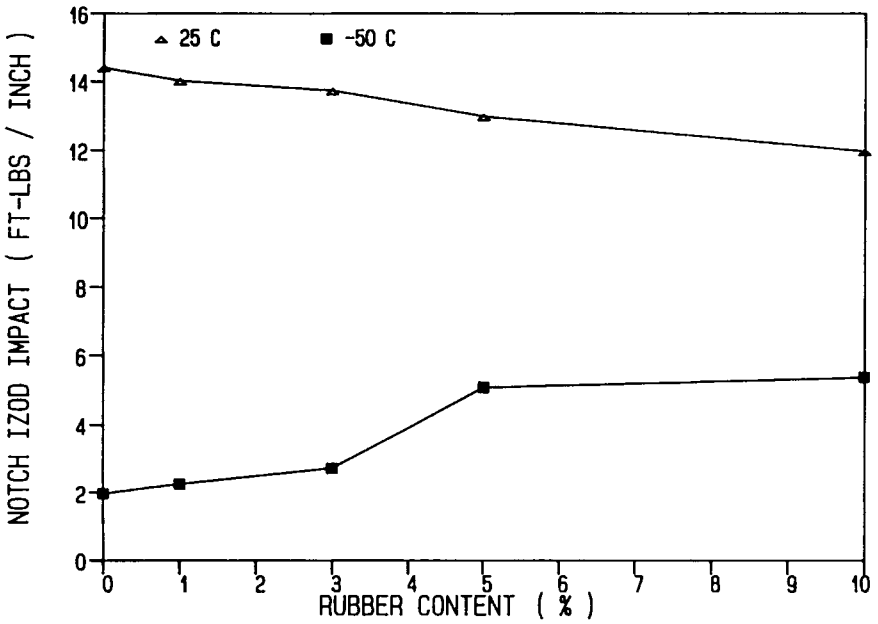

Figure 6 Effect of MBS elastomer content on the impact strength of PC in ductile and brittle fractures.

creased. Impact strength decreases with the increase of elastomer content if the fracture is in ductile mode (Figs. 4 and 6). To the contrary, the impact strength increases with the increase of elastomer content if the failure is in the brittle mode (Figs. 4 and 6). At temperatures below −80°C, below the T_g of the elastomer, essentially all the compositions approach a constant low impact strength.

Figure 7 exhibits the micrographs of the brittle-fractured surfaces of the elastomer-modified PCs. PC containing more elastomer exhibits more of the elastomer-initiated localized shear yielding corresponding to the higher impact strength observed in the brittle fracture. The plane-stress mass shear yielding, characterized with lateral contraction from the fractured surface, was not present in these brittle-fractured surfaces.

Figure 8 compares the impact strengths and the DBTTs from various MW PCs containing the same amount of elastomer (5%). The presence of 5% MBS elastomer reduces the PC DBTTs about 25°C for PCs MFR = 3, 15, and 22 and 50°C for PC MFR = 80.

Figure 9 exhibits the TEM photomicrographs of the PC (MFR = 15) modified with 10% MBS elastomer under various deformed states. Because of the dark-stained elastomer particles and the good adhesion between the elastomer and the PC matrix, the degrees of the elastomer deformation can be used to estimate the matrix extension ratio.

Figure 9(a) is the morphology of the specimen directly out of injection molding where the large elastomer particles have already been deformed with $R/r = 2$. Shearing and quenching effects during injection molding cause polymer chain orientation and elastomer distortion. Figure 9(b) shows the morphology of the yielding zone (but below the surface) of the ductile-fractured surface (fracture at ambient conditions). The elastomer particles are further elongated through the ductile fracture process, and the R/r ratio is now increased from the previous 2 to about 4. Since the direction of yielding during impact and the direction of melt flow during injection molding are not expected to be exactly the same, a minimum extension ratio of at least 2 through the ductile tearing fracture is thus assessed. Extension ratios between about 1.5 and 2.5 (60% of theoretically predicted maximum extension ratio) within the shear yield zone ahead of cracks for a wide range of polymers were previously reported.[46-48] For PC, the theoretically predicted maximum extension ratio was reported as 2.5.[46] Since the R/r ratio from the TEM photomicrograph does not necessarily come from the plane parallel to the maximum yielding direction, the R/r ratios obtained from TEM micrographs here, therefore, should be less or, at most, equal to the true maximum values. Figure 9(c) is the morphology of the whitening-yielded zone (but below the surface) from a brittle-fractured surface (fracture at −50°C) where the suspected elastomer-

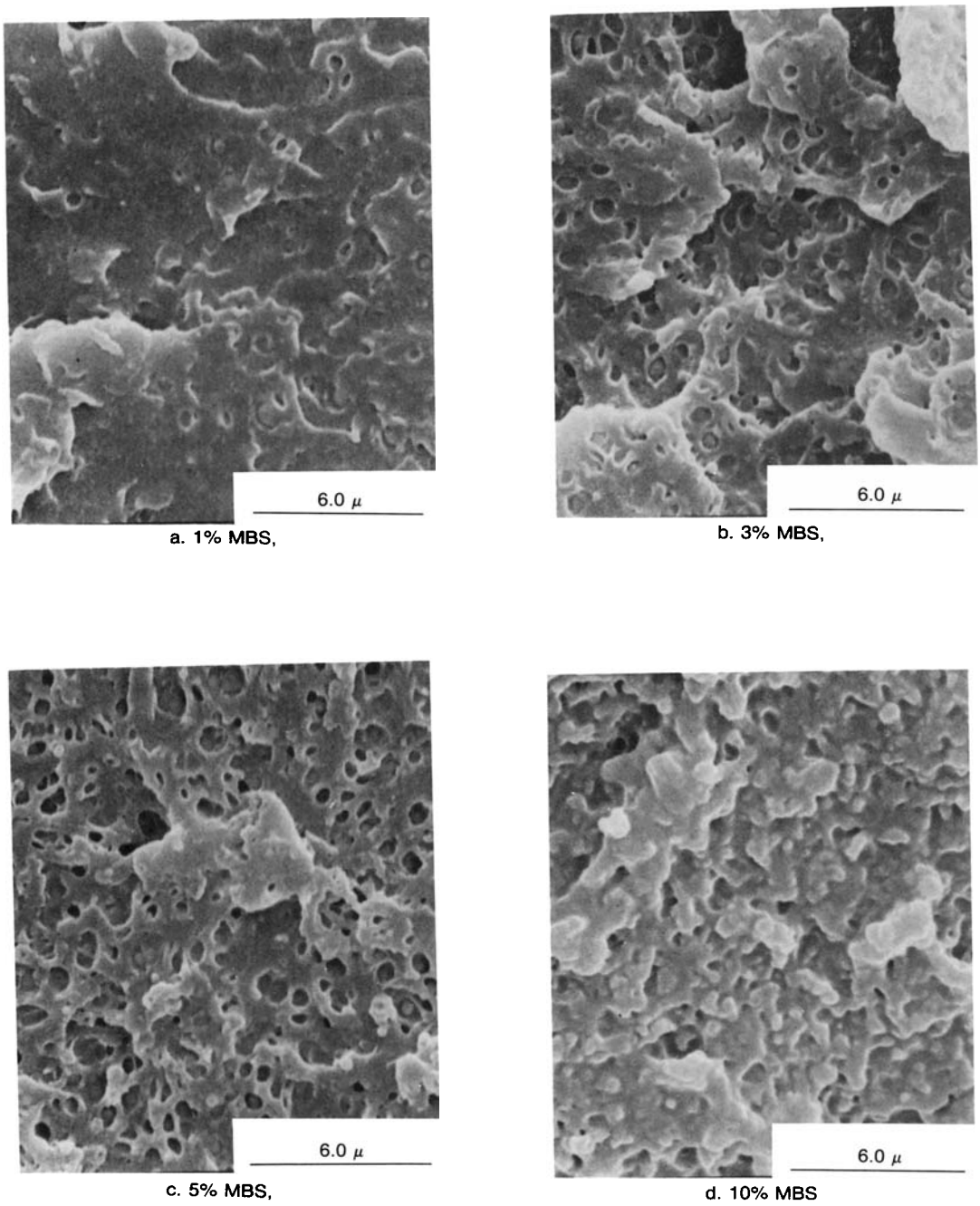

Figure 7 SEM microphotographs of brittle-fractured surfaces for PC MFR = 15 containing various amount of MBS elastomer ×4,000 at −60°C. (a) 1% MBS; (b) 3% MBS; (c) 5% MBS; (d) 10% MBS.

induced crazes are absent and the elastomer particles are highly deformed with R/r ratio about 10.

The absence of crazes in the above TEM micrographs does not prove or disprove that the crazes did not form in the yielding zone below the surface. The direction of the microtome slicing was carried out at the same direction as the possible crazes propagation. Based on the same assumptions mentioned above, the matrix yielding has an extension ratio of about 5 through brittle fracture. Such an observed extension ratio from the brittle fracture is significantly higher than the maximum extension ratio of 2.5 derived from a simple model in which the entanglement points are assumed to act as per-

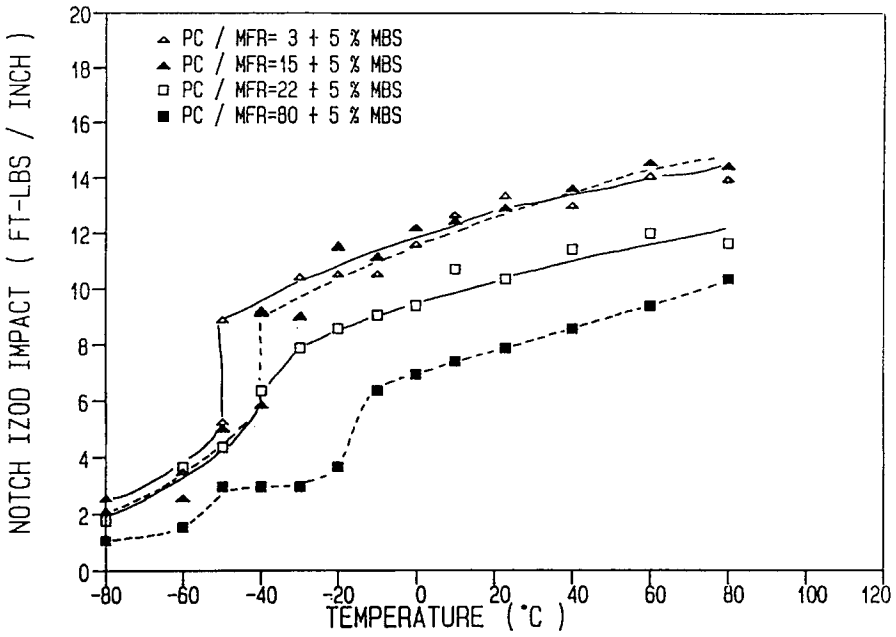

Figure 8 Izod impact strengths of various PC MFR containing 5% MBS elastomer.

manent cross-links with no chain slippage or scission occurring. Therefore, during brittle fracture with localized shear yielding, disentanglements and chain scissions appear to be involved. Comparing the estimated matrix extension ratios of the yielded zones from the ductile and the brittle-fractured surfaces, it is quite clear that the energy dissipation densities are not the same from these two types of fractures. The original purpose to investigate the TEM morphologies of this whitening-yielded zone was to check if any multiple crazes or microvoids were formed in the whitening zone of the brittle-fractured surface that might be partially responsible for the higher impact strength than that of the original PC. The obtained results can confirm only that the presence of elastomer promotes localized shear yielding to greater extents.

Impact Fracture Mechanics

The conventional Izod or Charpy impact testing involves the measurement of an energy, W, to break a notched specimen, and this is generally divided the ligament area A to give an apparent surface energy W/A. It is well known that such analysis of the data is not satisfactory since the parameter has a strong geometry dependency. LEFM, or its modified version, originally developed for metals has been widely and successfully applied to many brittle glassy polymers by the concept of a critical energy release rate, G_c, with a stable growth of cracking of a prenotched specimen. The G_c derived here is from the basic fracture mechanics in terms of energy absorbed at fracture. The specimen is also assumed to deform in a totally elastic manner so that the compliance, C, is a function only of crack length and the geometry. Thus, for an applied load P resulting in deflection x, we have the following relation:

$$\frac{x}{P} = C(a) \tag{1}$$

where a is the crack length. The energy absorbed, W, will be the area under the triangular load-displacement diagram:

$$W = \frac{1}{2} \times P \times x = \frac{1}{2} \times P^2 \times C \tag{2}$$

For a specimen of uniform thickness, B, the strain energy release rate, G, is given as

$$G = \frac{1}{B} \times \frac{dW}{da} \tag{3}$$

when $G = G_c$, a critical value, the elastic and brittle fracture occurs:

$$G_c = \frac{P^2}{2B} \times \frac{dC}{da} \tag{4}$$

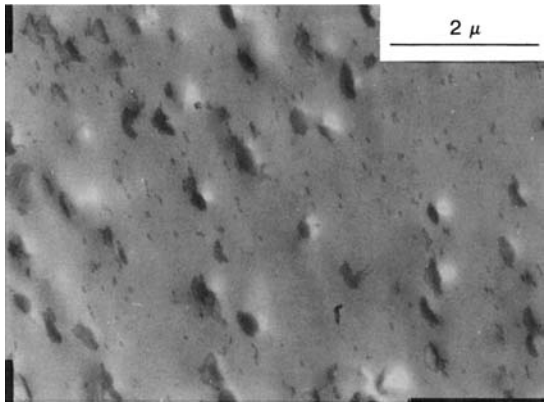

a. injection molded specimen prior to impact testing

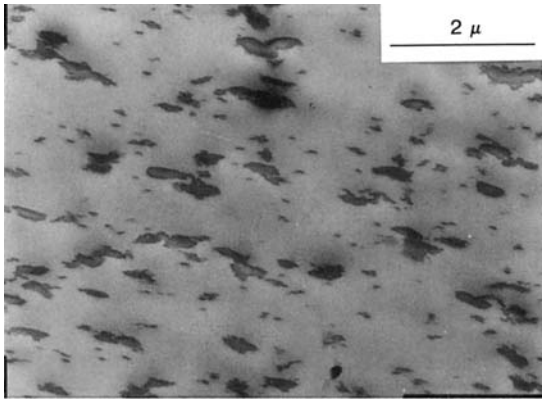

b. yielding zone in the ductile fractured surface (25°C)

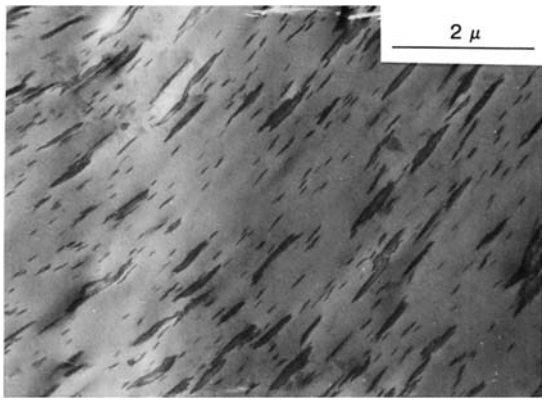

c. yield zone in the brittle fractured surface (−60°C)

Figure 9 TEM microphotographs (×10,000) of PC MFR = 15 containing 10% MBS elastomer under different deformed states: (a) injection-molded specimen prior to impact testing; (b) yielding zone in the ductile-fractured surface (25°C); (c) yielding zone in the brittle-fractured surface (−50°C).

From eqs. (2) and (4), we obtain

$$W = G_c \times B \times D \times \phi \tag{5}$$

where D is the specimen width and

$$\phi = \frac{C}{dC/d(a/D)} \tag{6}$$

If ϕ is determined as function of (a/D) and the energy measured at fracture is plotted as function of $B \times D \times \phi$ for different geometries, a straight line of slope G_c should result. ϕ may be determined experimentally or calculated theoretically, which has been verified on both Izod and Charpy methods.[49] The major error in this method is that the measured energy usually includes the kinetic energy of the specimen that can be found from the intercept of plotting W vs. $B \times D \times \phi$. Figure 10 shows the explanatory plots of the impact energies vs. $B \times D \times \phi$ for PC MFR = 15 with and without containing the 5% MBS elastomer. G_c are calculated from the slopes of the graphs from typically 25–35 specimens of various notch lengths. The fracture energy of the 5% MBS-modified PC (MFR = 15) is about twice that of the unmodified one. Figure 11 shows the plot of the PC number-average molecular weight (M_n) vs. G_c at −30°C. PC ($\frac{1}{8}$ in.) usually fails in a plane-stress ductile mode at the standard notch radius (10 mil) and ambient conditions. Under the purposedly chosen temperature (−30°C) and sharper notch radius (5 mil), the PCs and the elastomer-modified PCs fracture in a crazing-crack mode.

Flory[50] first suggested that some of the physical properties of polymers could be related to the number-average molar mass, M_n, by an empirical equation of the form

$$P = A - B/M_n \tag{7}$$

Figure 11 indicates that the M_n for zero G_c is about 6800 (equivalent to MFR = 135), which is very close to the previously reported value of 7500 derived from the tensile fracture stress.[30] Importance of entanglements in a polymer network in controlling the deformation behavior has been well recognized. Both fracture stress (σ_f) and fracture energy (G_c) fall to very low levels as M → Me. This corresponds to a value of molar mass, M_e, when the effective entanglements start to be formed in a polymer melt. In a normal MW distribution, the polymers with higher MW have less fraction of the molecules under M_e

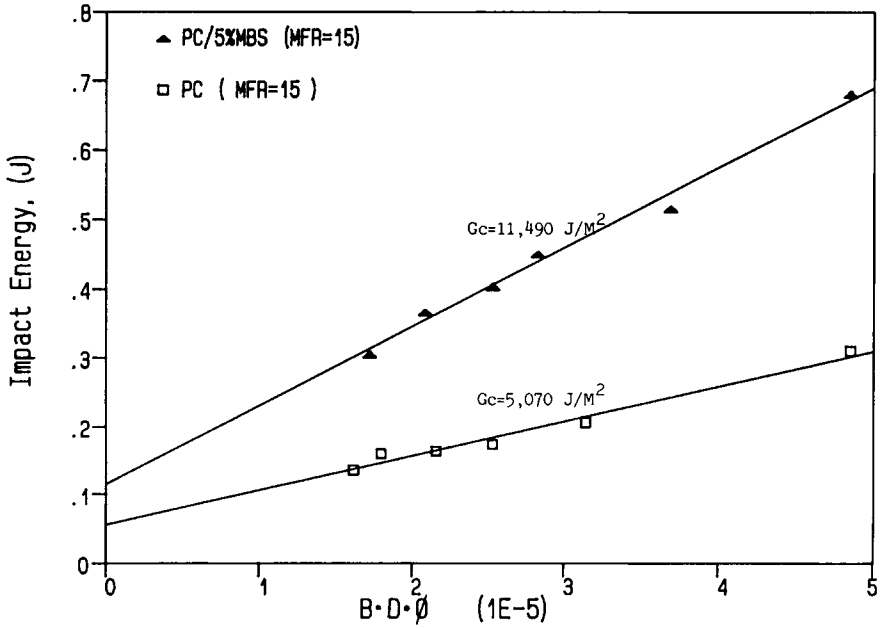

Figure 10 Plots of impact energy vs. $B \times D \times \phi$ for PC MFR = 15 with and without containing 5% MBS elastomer at −30°C.

and thus have a higher concentration of entanglements. Unlike other polymeric matrices, PC is much more molecular-weight-sensitive in terms of mechanical and rheological properties. Under the chosen experimental conditions, the plane-stress mass shear yielding does not occur while the less energy absorbing mechanisms such as the plane-strain localized shear yielding, crazing, and cracking are believed involved. The presence of elastomer in the PC matrix promotes the extent of these localized energy-absorbing mechanisms during fracture and results in higher fracture energy.

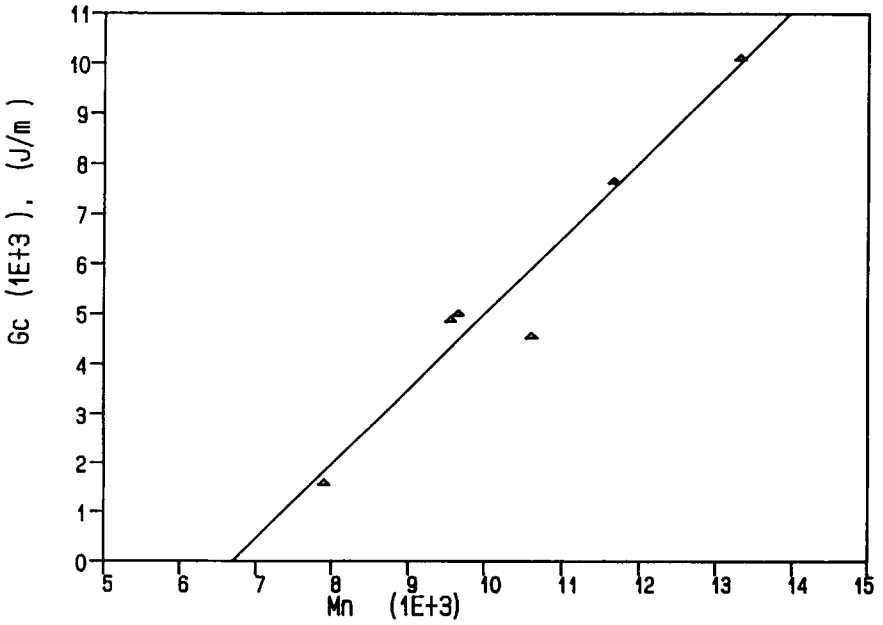

Figure 11 Plots of fracture energy at −30°C vs. number-average molecular weight of PC.

Elastomer Toughening Mechanism

The notched fracture process is highly complex in many ways. The stress distribution across the section is nonuniform. The presence of a notch produces stress concentration and a triaxial stress state below the notch. Tresca yield criterion predicts that the stress in the plastic zone under plane–stress conditions is the uniaxial yield stress, σ_y. The stress increases to $\sigma_y + \sigma_2$ under plane–strain conditions since the σ_2 is the smallest principal stress. The presence of elastomer above its T_g is able to relieve the yield stress increase caused by the plane–strain conditions. The presence of elastomer particles to enhance shear yielding is believed the main toughening mechanism. The observed impact strengths under various temperatures strongly suggest that the elastomer particles promote both the plane–strain localized and the plane–stress mass shear yielding. In case of the brittle failure at low temperatures, the fractured surface shows no sign of lateral contraction (indication of plane–stress mass shear yielding); instead, it is covered with a noticeable stress-whitening zone. Above the transition temperature, the lateral contraction starts to appear and the size is progressively increased with the increase of temperature and, therefore, the impact strength.

It appears that two modes of elastomer toughening mechanisms, localized and mass shear yielding, function simultaneously. The plane–strain localized shear yielding involves a volume much smaller than the plane–stress mass shear yielding. At low temperature (but above T_g of the elastomer) and brittle fracture, the plane–strain localized shear-yielding mechanism dominates the toughening process. When the temperature is increased to the transition, the plane–stress mass shear yielding begins to appear while the localized shear yield still plays an important role within the whole fracture process. As the temperature is continuously raised above the transition, the plane–stress mass shear yielding gradually becomes the dominant mechanism.

These two modes of elastomer-toughening mechanisms are probably not totally independent, but, rather, interrelated to some extent. The extension ratio of 5 from the brittle fracture vs. 2 from the ductile tearing further supports the proposed dual-mode system. The single most important factor in determining the ductile–brittle transition is the strain at crack initiation, and any effort to toughen pseudoductile matrices is to delay or retard crack initiation for allowing the growth of the precrack plastic zone over its critical value.[18,19,22,23,32,44] The concept of a critical plastic zone is proposed to interpret the ductile–brittle transition behavior was previously proposed.[44]

CONCLUSIONS

1. Polycarbonate density, yield stress, and modulus increase slightly with the decrease of its MW and elastomer content.
2. The impact DBTT decreases with the increase of the PC MW and elastomer contents.
3. The elastomer-modified PC has higher impact strength than does the unmodified one if it fails in brittle mode, but has lower impact strength if it fails in ductile mode.
4. Two separate modes, plane–strain localized and plane–stress mass shear yielding, function simultaneously in this elastomer-toughening mechanism. The elastomer-initiated localized shear yielding dominates the fracture process at low temperature and brittle failure, whereas the mass shear yielding dominates at higher temperature and ductile failure.
5. The extension ratio of the ductile tearing zone is about 2 compared with about 5 from the brittle-whitening zone for the 10% MBS-modified PC. Therefore, the energy dissipation density of the plane–stress yielding zone of the ductile fracture is less than the plane–strain localized yielding zone of the brittle fracture.
6. The criteria for polycarbonate brittle or ductile fracture is the size of precrack plastic zone. The crack initiation strain is the most important factor in determining the size of precrack plastic zone and thus the mode of fracture.

This study was supported by the National Science Council, Republic of China, under contract number NSC 78-0405-E-009-03.

REFERENCES

1. A. J. Kinlock and R. J. Young, *Fracture Behavior of Polymers,* Elsevier, London, 1983.
2. C. B. Bucknall, *Toughened Plastics,* Applied Science, London, 1977.
3. D. R. Paul, J. W. Barlow, and H. Keskkula, *Encyclopedia of Polymer Science and Engineering,* Wiley, New York, 1988, Vol. 12, 2nd ed.

4. G. L. Pitman, I. M. Ward, and R. A. Duckett, *J. Mater. Sci.*, **13,** 2092 (1978).
5. W. E. Wolstenholme, S. E. Pregun, and C. F. Stark, *J. Appl. Polym. Sci.*, **8,** 119 (1964).
6. J. Heijboer, *J. Polym. Sci. C,* **16,** 3755 (1968).
7. G. Allen, D. C. W. Morley, and T. Williams, *J. Mater. Sci.*, **8,** 1449 (1973).
8. E. Pleti and J. G. Williams, *Polymer,* **16,** 915 (1975).
9. R. Ravetti, W. W. Gerberich, and T. E. Hutchinson, *J. Mater. Sci.*, **10,** 1441 (1975).
10. M. Parvin and J. G. Williams, *J. Mater. Sci.*, **10,** 1883 (1975).
11. N. J. Mills, *J. Mater. Sci.*, **11,** 363 (1976).
12. J. T. Ryan, *Polym. Eng. Sci.*, **18,** 264 (1978).
13. S. Havriliak, Jr. and V. E. Malpass, *S.P.E. ANTEC Tech. Papers,* **31,** 645 (1985).
14. R. H. Shoulberg and J. J. Gouza, *SPE J.*, **23,** 32 (1967).
15. F. C. Chang and L. H. Chu, *Proc. of ACS Div. Polym. Mater.: Sci. Eng.*, **60,** 851 (1989).
16. F. C. Chang and L. H. Chu, *J. Appl. Polym. Sci.*, to appear.
17. C. K. Riew and R. W. Smith, in *Rubber-toughened Plastics,* C. K. Riew, Ed., Advances in Chemistry 222, American Chemical Society, Washington, D.C., 1989, p. 225.
18. H. C. Hsu and F. C. Chang, in *Proceedings of the 1990 Annual Conference of the Chinese Society for Material Science,* Taipei, 1990, p. 1005.
19. F. C. Chang and H. C. Hsu, in *Proceedings of the China-Japan Bilateral Symposium,* Guangzhou, China, September 1990.
20. A. F. Yee, *J. Mater. Sci.*, **12,** 757 (1977).
21. M. E. Dekkers and S. Y. Hobbs, *Polym. Eng. Sci.*, **27,** 1164 (1987).
22. F. C. Chang and H. C. Hsu, *Proc. ACS Div. Polym. Mater.: Sci. Eng.*, **62** (1990).
23. H. C. Hsu and F. C. Chang, *Proceedings of the 13th ROC Polymer Symposium,* Taiwan, 1990, p. 796.
24. D. G. Legrand, *J. Appl. Polym. Sci.*, **13,** 2129 (1969).
25. G. A. Adam, A. Gross, and R. N. Haward, *J. Mater. Sci.*, **10,** 1582 (1975).
26. F. C. Chang and L. H. Chu, IUPAC, Korea, 105 (1989).
27. C. B. Crowet and J. C. Bauwens, *Polymer,* **27,** 709 (1986).
28. K. S. Kim and F. C. Chang, in *Proceedings of the 13th ROC Polymer Symposium,* Taiwan, 1990, p. 24.
29. L. H. Chu and F. C. Chang, in *Proceedings of the 12th ROC Polymer Symposium,* Taiwan, 1989, p. 519.
30. J. H. Golden, B. L. Hammant, and E. A. Hazell, *J. Polym. Sci. A,* **2,** 4787 (1964).
31. J. A. Brydson, *Plastics Materials,* 4th ed., Butterworth Scientific, London, 1965, p. 507.
32. F. C. Chang and H. C. Hsu, *J. Appl. Polym. Sci.*, to appear.
33. S. Newman and S. Strella, *J. Appl. Polym. Sci.*, **9,** 2297 (1965).
34. R. P. Petrich, *Polym. Eng. Sci.*, **13,** 248 (1973).
35. F. Haaf, H. Breuer, and J. Stabenow, *J. Macromol. Sci. Phys.*, **B-14,** 387 (1977).
36. S. Wu, *Polymer,* **26,** 1855 (1985).
37. S. Y. Hobbs, R. C. Bopp, and V. H. Watkins, *Polym. Eng. Sci.*, **23,** 380 (1983).
38. S. Wu, *J. Appl. Polym. Sci.*, **35,** 549 (1988).
39. U. S. Pat., 4,122,131 (October 24, 1978).
40. U. S. Pat., 4,562,222 (December 31, 1985).
41. U. S. Pat., 4,564,655 (January 14, 1986).
42. U. S. Pat., 4,737,545 (April 12, 1988).
43. S. Wu, *J. Polym. Sci. Polym. Phys. Ed.*, **21,** 699 (1983).
44. F. C. Chang and M. Y. Yang, *Polym. Eng. Sci.*, **30,** 543 (1990).
45. D. Hull and T. W. Owen, *J. Polym. Sci. Polym. Phys. Ed.*, **11,** 2039 (1973).
46. A. M. Donald and E. J. Kramer, *Polymer,* **23,** 1183 (1982).
47. A. M. Donald and E. J. Kramer, *J. Polym. Sci. Polym. Phys. Ed.*, **20,** 899 (1982).
48. A. M. Donald and E. J. Kramer, *J. Mater. Sci.*, **17,** 1765 (1982).
49. E. Plati and J. G. Williams, *Polym. Eng. Sci.*, 470 (1975).
50. P. J. Flory, *J. Am. Chem. Soc.*, **67,** 2048 (1945).

Received March 18, 1991
Accepted April 8, 1991